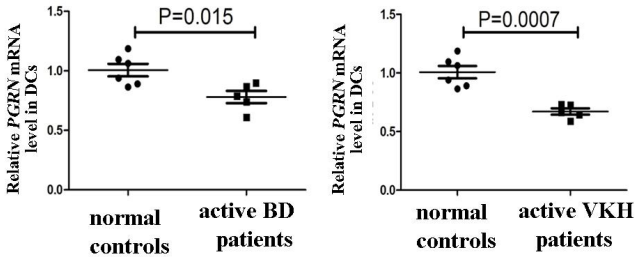

Figure e-1 The gene expression of PGRN in monocyte-derived DCs from aBD and aVKH patients. (5 aBD patients VS 6 normal controls, 5 aVKH patients VS 6 normal controls). Data are expressed as mean ± SEM and dots represent individual participants. Independent T tests were used for statistical analyses.

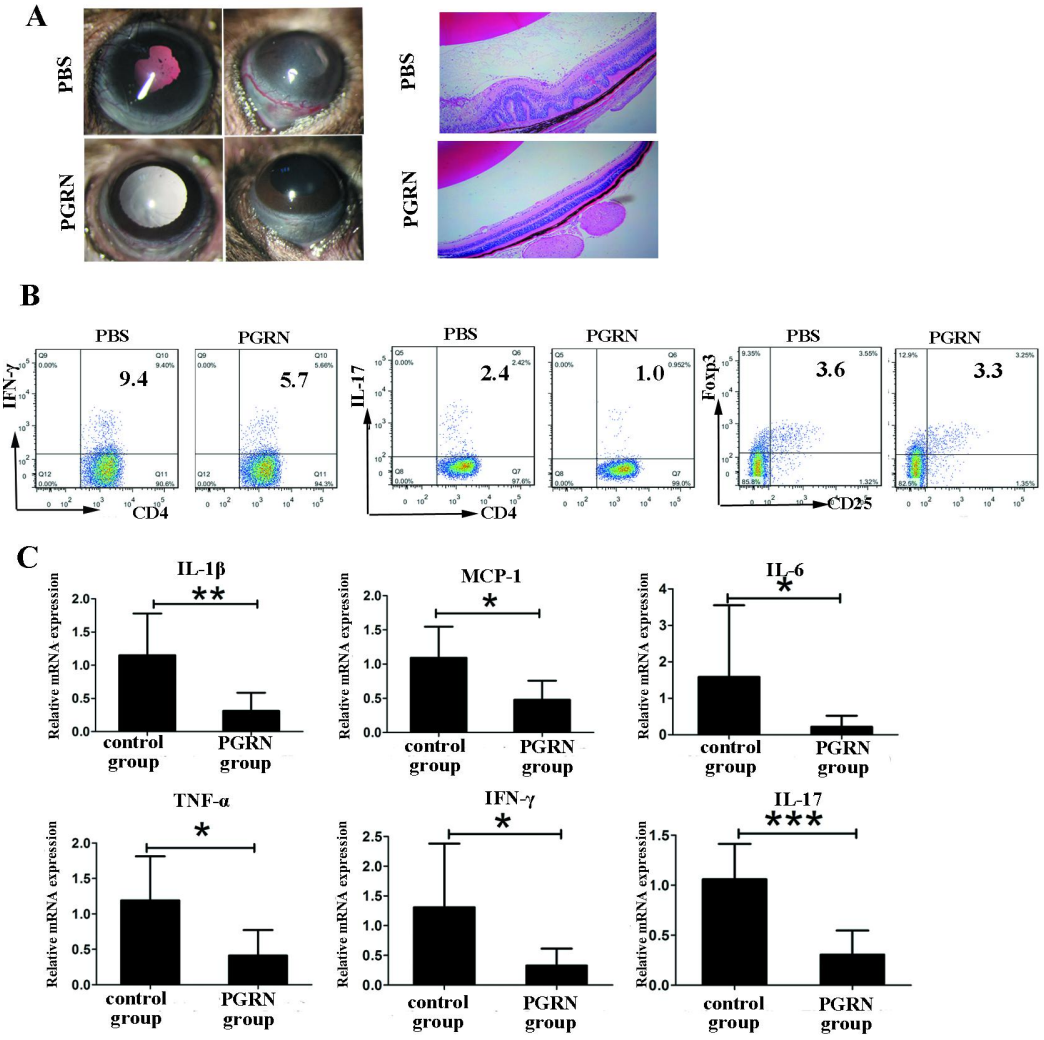

Figure e-2. PGRN attenuates EAU and inhibits Th1 and Th17 immune response. (A) B10RIII mice were immunized for EAU and injected intraperitoneally with rPGRN or PBS every other day from day 7 to 13 postimmunization. Representative slit-lamp images and histopathology of retina (original magnification 10×) the two EAU groups on day 13 postimmunization were shown respectively. (B) Dot plots of a representative subject of intracellular expression of IL-17, IFN-γ and $CD25^{+}Foxp3^{+}$ by $CD4^{+}$T cells in the spleen for each group. (C) Quantitative RT-PCR analysis of inflammatory cytokines in the retina from PGRN- or PBS-treated mice after immunization on day 13. Data shown as mean±SEM from 2- 3 independent experiments with total of 10 mice per group. *: $p < 0.05$, **: $p < 0.01$, ***: $p < 0.001$

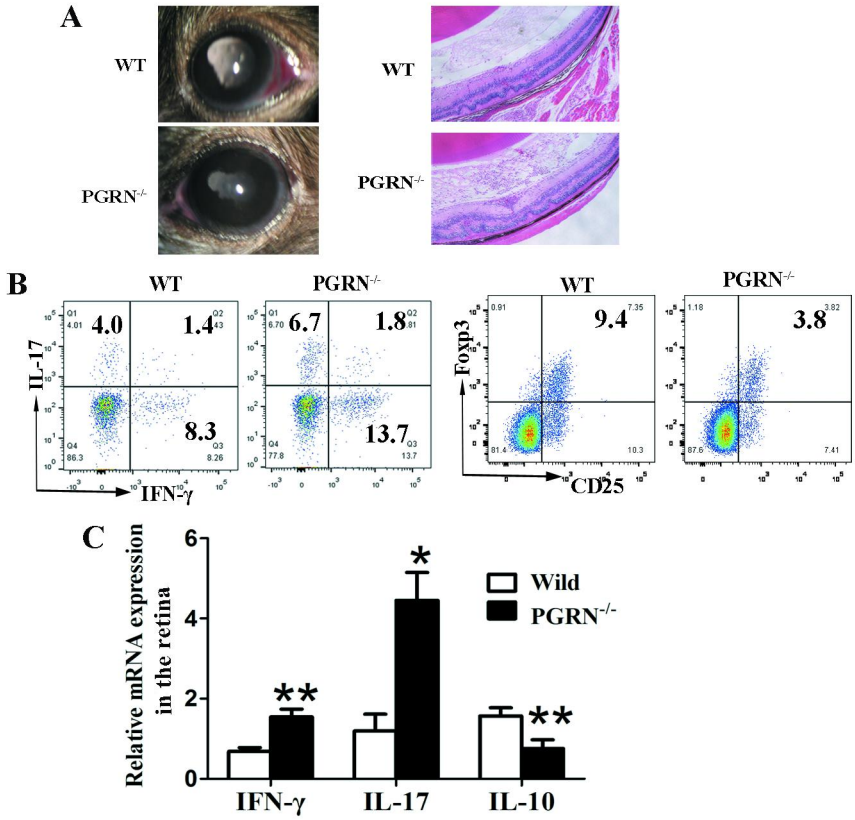

Figure 3. PGRN$^{-/-}$ mice develop exacerbated EAU. WT and PGRN$^{-/-}$ mice of C57BL/6 background were induced for EAU. (A)Representative slit-lamp images and representative histopathology (original magnification 10×) of retina from the two groups on day 13. (B) Representative flow cytometry dot plots of IL-17, IFN-γ and Foxp3 by CD4^{+}T cells for each group. (C) Quantitative RT-PCR analysis of INF-γ, IL-17 and IL-10 in the retina. Data shown as mean±SEM from 2- 3 independent experiments with total of 10 mice per group. *: $p < 0.05$, **: $p < 0.01$, ***: $p < 0.001$.

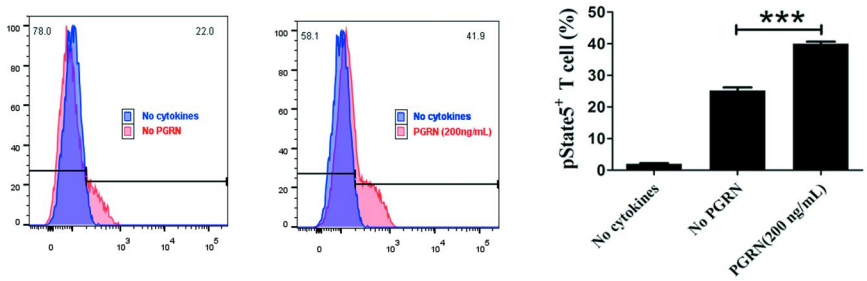

Figure 4. p-STAT5 was assessed on the Treg-polarized $CD4^+$ population in the presence or absence of PGRN by flow cytometry. Data shown as mean±SEM from 2 independent experiments. *: $p < 0.05$, **: $p < 0.01$, ***: $p < 0.001$.

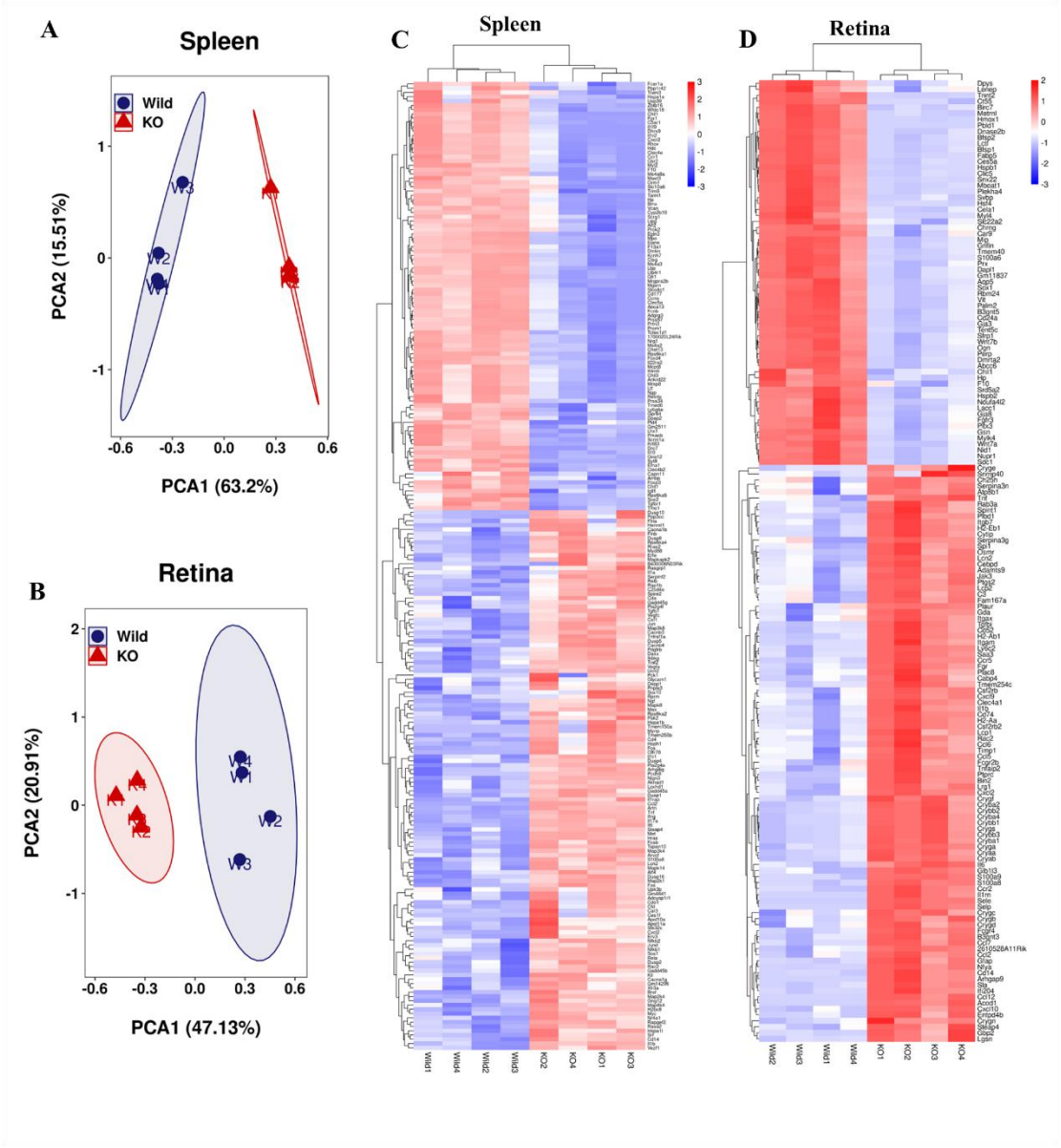

Figure e-5. DEG screening. (A-B) Principal component analyses (PCA) of gene expression in the (A) spleen and (B) retina between WT and PGRN$^{-/-}$ EAU group. (C-D) Heat map of DEGs. A total of 226 (126 upregulated and 100 downregulated) DEGs in the spleen and 160 (96 upregulated and 64 downregulated) DEGs in the retina were identified from PGRN-/- EAU mice as compared to WT EAU. In Figure C and D, the left four columns represent WT EAU group and the right 4 columns represent PGRN$^{-/-}$ EAU group. Each row represents a single gene. The color change from red to blue represents lg(FPKM+1) value ranging from high to low. Genes with same or similar expression pattern are linked by black lines.

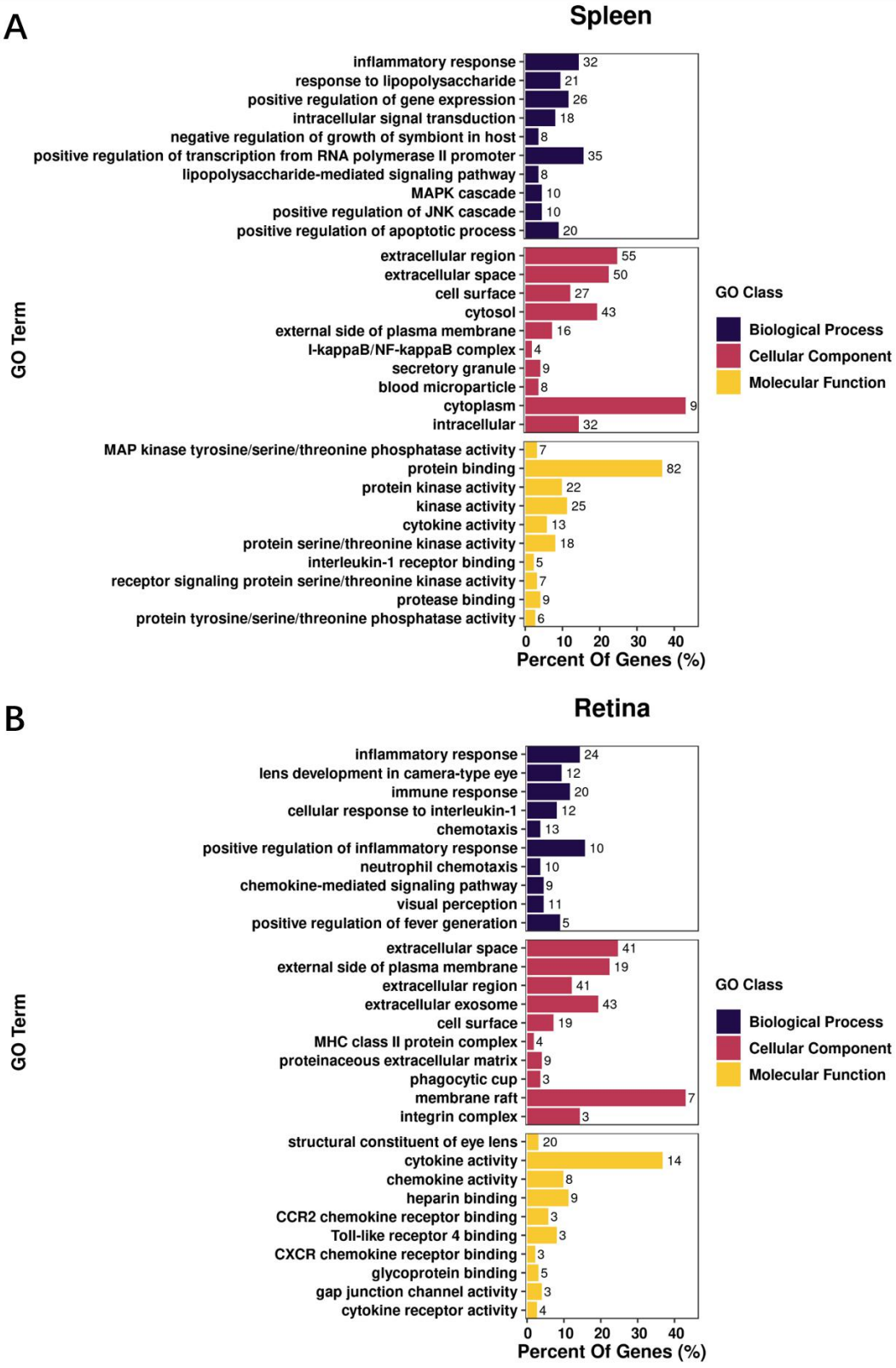

Figure e-6. Gene ontology (GO) enrichment analysis. GO analysis for DEGs in the (A) spleen and (B) retina between WT and PGRN$^{-/-}$ EAU group. The figure presents only the top 10 of significant GO enrichment items in different functional groups.

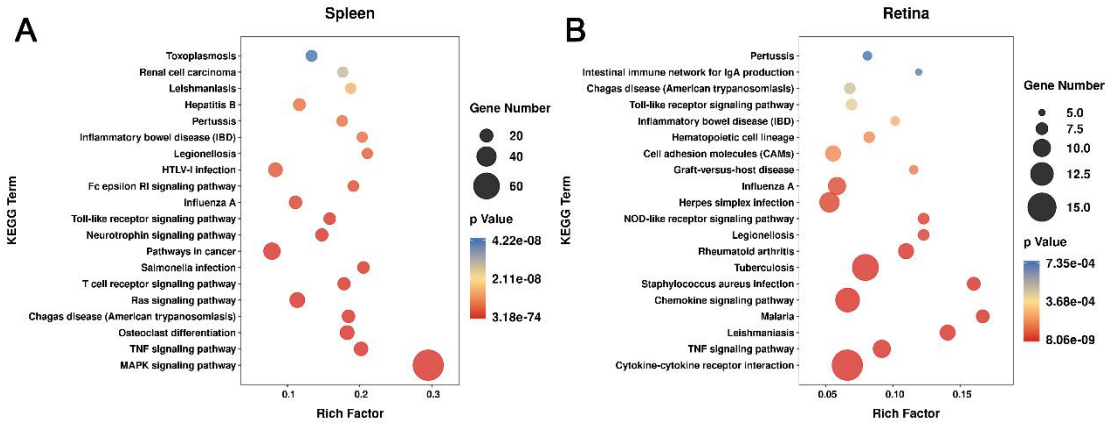

Figure e-7. KEGG enrichment analysis of DEGs in the (A) spleen and (B) retina between WT and PGRN$^{-/-}$ EAU group. The figure presents only the top 20 of significant KEGG enrichment items.

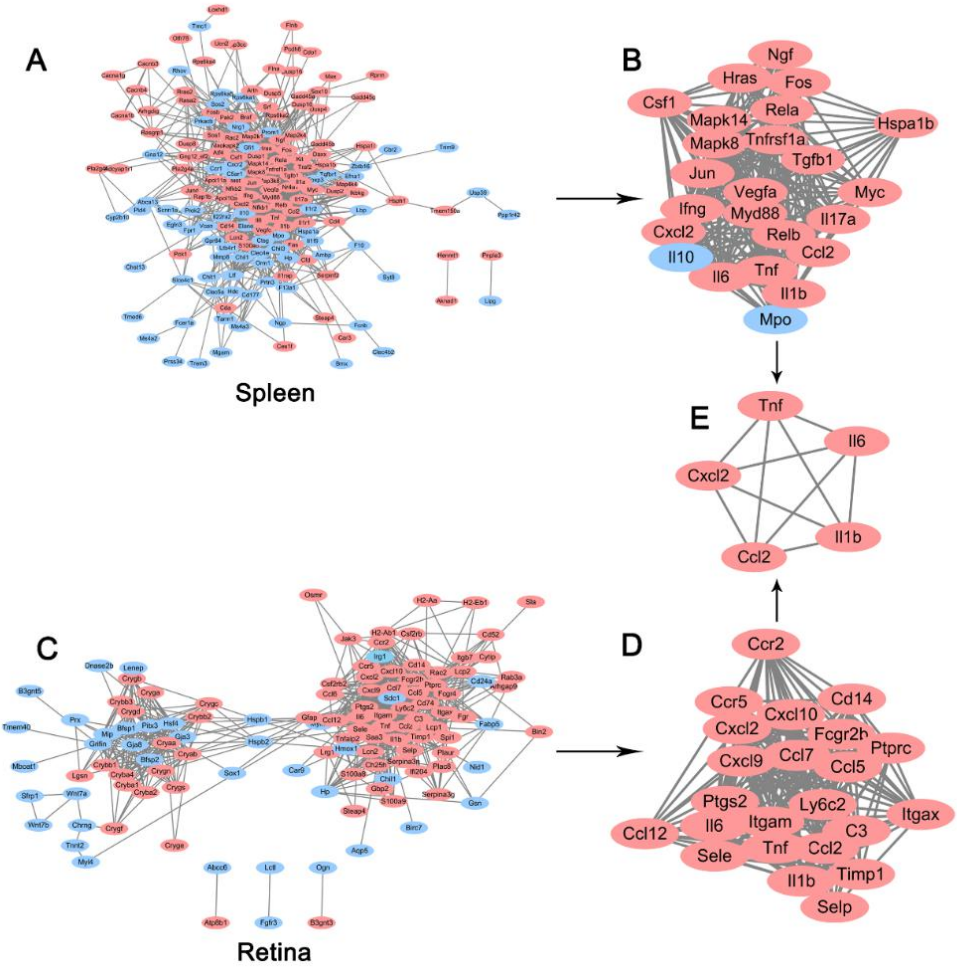

Figure e-8. PPI network construction and Module Analysis. The PPI network of DEGs in the (A) spleen and (C) retina between WT and PGRN$^{-/-}$ EAU group was constructed using Cytoscape. In the spleen, a PPI network containing 177 nodes (106 upregulated and 71 down-regulated) and 1179 edges was constructed. In the retina, a PPI network containing 120 nodes (80 upregulated and 40 down-regulated) and 766 edges was constructed. Hub genes were then screened and identified by Cytoscape MCODE (node degree of >10). (B) In the spleen, 24 hub genes were identified among the 177 nodes in the spleen, which were all upregulated genes except 2 genes (Il10 and Mpo). (D) In the retina, 23 hub genes among the 120 nodes were all upregulated. (E) 5 shared hub genes were found in both spleen and retina. Upregulated genes are marked in light red; downregulated genes are marked in light blue.

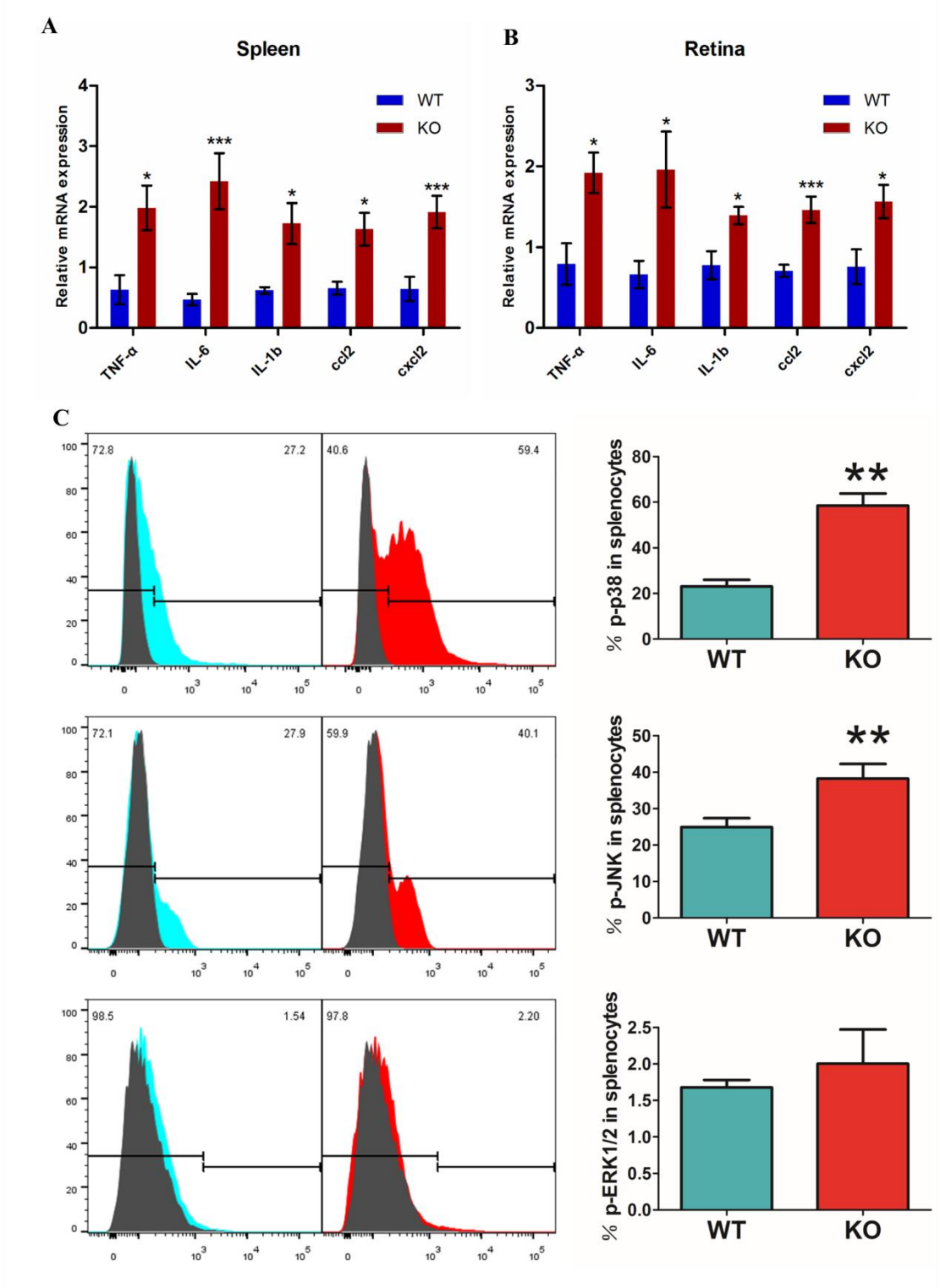

Figure e-9. Verification of the hub genes and MAPK signaling pathway. (A-B) The five shared hub gene expression in both the (A) spleen and (B) retina was detected by RT-PCR. (C) Flow cytometry analysis of phosphorylated levels of p38, JNK and ERK1/2 in splenocytes of WT and PGRN-/- EAU (WT: wildtype EAU, KO: PGRN-/- EAU 6 mice per group). Data are represented as mean±SEM. Compared with WT group, *$p < 0.05$, **$p < 0.01$, ***$p < 0.001$.

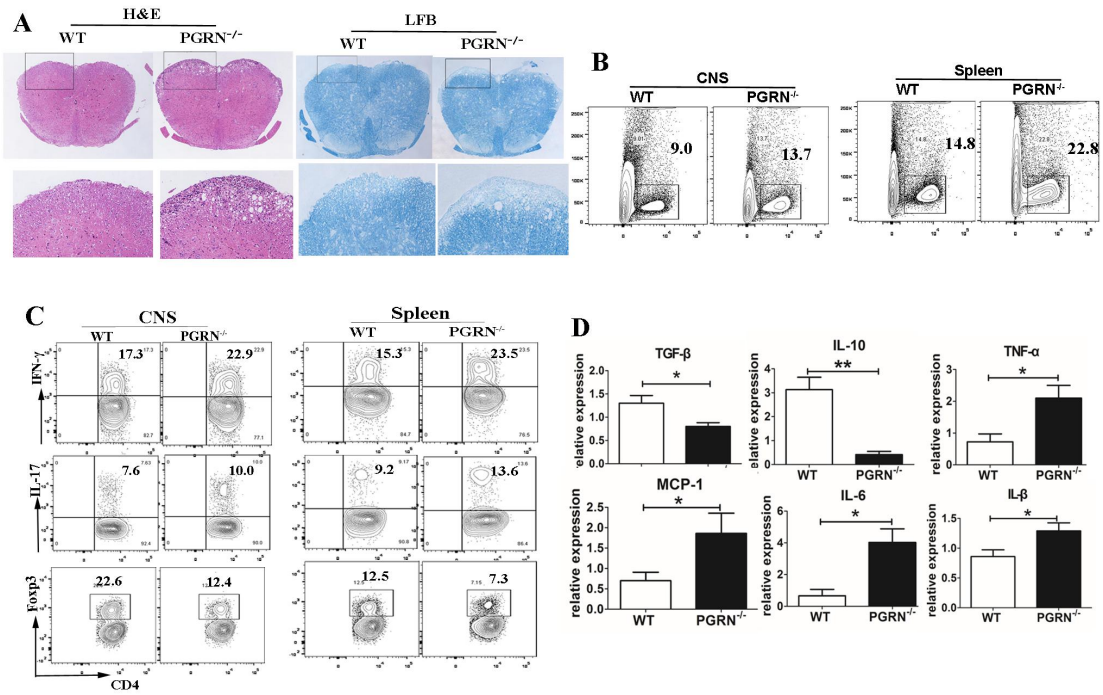

Figure e-10. PGRN$^{-/-}$ mice develop more severe EAE. WT and PGRN$^{-/-}$ mice of C57BL/6 background were induced for EAE. (A) Sections of spinal cord were obtained from the two group EAE mice at day 22 post immunization. Representative H&E staining and Luxol fast blue (LFB) staining of spinal cord sections (upper panel: original magnification 5×, under panel: original magnification 20×). (B) Detection of the frequency of CD4^{+}T cells in the CNS (brain and spinal cord) and spleen by flow cytometry, representative flow cytometry dot plots for each group are shown. (C) Detection of the frequency of INF-γ^{+}CD4^{+}T cells(Th1), IL-17^{+}CD4^{+}T cells(Th17) and Foxp3^{+}CD4^{+}T(Treg) cells in the CNS (brain and spinal cord) and spleen by flow cytometry, representative flow cytometry dot plots for each group are shown. (D) Quantitative RT-PCR analysis of MCP-1, TNF-α, IL-1β, IL-6, TGF-β and IL-10 in the spinal cord from WT EAE and PRGN$^{-/-}$ EAE mice. Data shown as mean±SEM from 3 independent experiments with total of at least 10 mice per group. *: $p < 0.05$, **: $p < 0.01$, ***: $p < 0.001$.

Table e-1 Primer sequences used for real-time PCR.

Gene	Sequences（5’- 3’）
TNF-α (forward)	AGGCGCCACATCTCCCTCCA
TNF-α (reverse)	CGGTGTGGGTGAGGAGCACG
IL-6 (forward)	AGATAACAAGAAAGACAAAGCCAGAGTC
IL-6 (reverse)	GCATTGGAAATTGGGGTAGGAAG
IL-1b (forward)	TTGAAGAAGAGCCCGTCC
IL-1b (reverse)	CTTATGTTCTGTCCATTGAGGT
Ccl2 (forward)	AGTTGCCGGCTGGAGCATCC
Ccl2 (reverse)	TCTTTGGGACACCTGCTGCTGG
Ccxl2 (forward)	TCCTCAATGCTGTACTGGTCC
Ccxl2 (reverse)	ATGTTCTTCCTTTCCAGGTC
GAPDH (forward)	TGAACGGGAAGCTCACTGG
GAPDH (reverse)	TCCACCACCCTGTTGCTGTA
NOS2 (forward)	ACCCACATCTGGCAGAATGAG
NOS2 (Reverse)	AGCCATGACCTTTCGCATTAG
Arg1 (forward)	CTTGGCTTGCTTCGGAACTC
Arg1 (Reverse)	GGAGAAGGCGTTTGCTTAGTTC

eMethods

Patients

Thirty-four active BD patients, 37 active VKH patients and forty age- and gender-matched healthy individuals were enrolled in this study. Neither systemic corticosteroids nor other immunosuppressive agents were used in the VKH/BD patients included in this study at least for two weeks before blood sampling. According to the staging system,[1, 2] there were 4,10 and 24 patients in posterior uveitis stage (within 2 weeks after uveitis onset), anterior uveal involvement stage (between 2 weeks and 2 months after disease attack) and in the recurrent period of granulomatous anterior uveitis (over 2 months after disease onset) respectively. All the patients fulfilled the international criteria for the diagnosis of BD [3] and VKH [4, 5] respectively. In this study, aBD was defined as active aqueous inflammation and/or vitreous cells, retinitis or retinal vasculitis. The active VKH patients defined either as diffuse choroiditis associated with serous retinal detachment in the early stage, or as mutton fat KP, aqueous cells and flare, iris nodules, and sunset glow fundus in the late stage.

EAU Induction and clinical activity evaluation

B10.RIII and C57BL/6 are normally used for induction of EAU and B10.RIII is the most sensitive strain to IRBP-induced EAU model.[6] Transgenic and knockout experiments are usually performed in C57BL/6 strain, whereas other experiments are widely carried out in B10.RIII mice. Different peptides in different concentrations are requested in these two strains of mice for the induction of EAU.[7, 8, 9] To determine the effect of rPGRN on uveitis, EAU was induced in B10RIII mice according to the method described previously.[9] In brief, the B10RIII mice (Jackson Laboratories) were immunized at the base of the tail and both thighs with 50μg human $IRBP_{161-180}$ peptide ((Shanghai, China) in 100 mL PBS emulsified with an equal volume of complete Freund's adjuvant (CFA) (Sigma-Aldrich, St. Louis, MO) containing 1.0 mg/mL *Mycobacterium tuberculosis* strain H37Ra (Sigma-Aldrich). Mice were randomized into 2 groups, the mice receiving PGRN (5μg/100ul, R&D systems) intraperitoneal injection every other day from day 7 to 13 after the initial immunization serve as PGRN-treated EAU group. The dose of PGRN used in this study was based on that reported in previous studies.[10, 11] while control WT EAU group received equal volume of

PBS in the same manner. Clinical signs of EAU were assessed by slit-lamp microscopy in a masked manner by two independent observers and scored on a scale of 0 to 5 [9]. Eyes were harvested on day 13 and then processed for histopathological assessment in a masked manner (0 to 4 scales).[12]

The effect of PGRN deficiency on EAU was evaluated in WT or $PGRN^{-/-}$ mice of C57BL/6 background (Jackson Laboratories). Briefly, mice were immunized subcutaneously with 400 μg human $IRBP_{651–670}$ (LAQGAYRTAVDLESLASQLT) in 100μl PBS emulsified with an equal volume of CFA containing 5 mg/ml *Mycobacterium tuberculosis* strain and received intraperitoneal injection of 1 μg Bordetella pertussis toxin (Sigma-Aldrich) as previously described.[7] Clinical manifestation and histopathological change were evaluated according to the method described previously.[7] All experimental animals were maintained in a specific pathogen-free facility at the Chongqing Medical University.

EAE Induction, clinical activity and CNS histopathology evaluation

To determine the role of PGRN in EAE development, WT or $PGRN^{-/-}$ mice of C57BL/6 background (Jackson Laboratories) were used for this model. In brief, mice were immunized subcutaneously with 300 μg MOG35–55 (MEVGWYRSPFSRVVHLYRNGK) emulsified in CFA supplemented with 5 mg/mL of *Mycobacterium tuberculosis* strain. Pertussis toxin (200 ng in 100 ul PBS for each time) was injected intraperitoneally on day 0 and 2 post-immunization. EAE was assessed daily for symptoms in a masked manner by two independent observers and scored using a scale from 0 to 5 as previously described[13]. The mice were also regularly monitored for body weight changes.

For histopathological evaluation, mice were extensively perfused on day 22 p.i. with PBS and fixed with 4% (wt/vol) paraformaldehyde via the heart to eliminate peripheral blood. The spinal cords were collected and stained with luxol fast blue (LFB) for demyelination detection and H&E for inflammation assessment in a masked manner as described earlier.[14]

For analysis of the local immune response in the spinal cord and brain, the mice were perfused on day 22 p.i., and infiltrating mononuclear cells were harvested from the spinal cord and brain according to the methods described earlier.[14] The harvested cells were detected for the frequency

of Th1/Th17/Treg and M1/M2macrophages.

Cell culture

To investigate the effect of rPGRN on the IRBP peptide–induced Th1/Th17/Treg cell immune response in vitro, spleen cells from EAU mice on day 13 were cultured in 24-well plates at $4x10^6$/2 ml per well and stimulated with $IRBP_{651–670}$ peptide (10ug/ml) in the presence or absence of rPGRN(200ng/ml, R&D Systems). At 72h, the cells were harvested and pulsed with PMA/Ionomycin for the detection of Th1, Th17 and Treg by flow cytometry.

To examine the effects of PGRN on Th1/Th17/Treg cell response undergoing polarization from naive $CD4^+$T cells respectively in vitro, naive $CD4^+$T cells from the spleen of normal C57BL/6 mice were stimulated with anti-CD3 (5 μg/ml)/CD28 (1 μg/ml) in the presence or absence of rPGRN (200ng/ml) in 48-well plates at $2x10^5$/ml. For Th1 polarization, cultures were supplemented with IFN-γ (10ng/ml) and IL-12 (10 ng/ml) at the time of plating. For Th17 cell polarization, the cultures were supplemented with TGF-β (2.5ng/ml), IL-6 (25ng/ml), IL-23(10ng/ml), anti-IFN-γ（10ug/ml）and anti-IL-4 (10ug/ml) at the time of plating. For Treg cell polarization, the cultures were supplemented with TGF-β（5ng/ml）at the time of plating. At 72 h after culture, the cells were harvested and pulsed with PMA/Ionomycin and stained for intracellular cytokine analysis of Th1/Th17/Treg or p-STAT5 by flow cytometry. All the antibody and recombinant protein for Th cell polarization were from Biolegend or BD Biosciences.

To study the role of PGRN in the macrophage polarization, bone marrow cells were isolated from the femur and tibia of normal C57BL/6 mice and were cultured with M-CSF (20ng/ml, PeproTech) for 7 days. These differentiated M0 macrophages were harvested and plated in 48-well plates at a density of 1 $x10^6$ cells/well, and then cultured with or without PGRN(200ng/ml) in the presence M1 polarizing conditions (LPS (100ng/ml, Sigma-Aldrich) and IFN-γ（20ng/ml, R&D Systems)) or M2 polarizing conditions (IL-4 (25ng/ml, R&D Systems)) for 48h. The cells were harvested and analyzed for the expression of inducible nitric oxide synthase (iNOS) and arginase 1(Arg-1) by RT-PCR.

RNA-sequencing (RNA-seq) and screening of differentially expressed genes (DEGs)

On day 13 postimmunization, the spleen and retina from WT EAU group and PGRN$^{-/-}$ EAU group were subjected to RNA-seq. Total RNA was isolated from the spleen and retina using Trizol Reagent. RNA-seq analysis was performed in Bio-tree Technology Inc., shanghai, China. RNA-seq was carried out with the PE150 sequencing strategy by the Illumina Novaseq 6000 platform. DEG analysis between the WT EAU and PGRN$^{-/-}$ EAU group was performed using the DESeq2 R package (1.16.1).[15] The resulting P-values were adjusted using the Benjamini and Hochberg's approach for controlling the false discovery rate. Genes with an adjusted P-value <0.05 and |log2foldchange|>1 found by DESeq2 were assigned as differentially expressed.

Gene Ontology (GO) analysis, Kyoto Encyclopedia of Genes and Genomes (KEGG) pathway Analysis and Gene set enrichment analysis (GSEA)

The GO database (http://www.geneontology.org) provides functional classification for genomic data, including categories of biological processes (BP), cellular component (CC), and molecular function (MF).[16] KEGG is a bioinformatics database for understanding the functions and utilities of cells and organisms from molecular-level information, especially large-scale molecular datasets generated by genome sequencing and other high-through put experimental technologies (http://www.genome.jp/kegg/).[17] GO and KEGG pathway enrichment analysis were performed on DEGs using the DAVID database to enrich significantly altered pathway.[18] FDR<0.05 was set as the cut- off criterion for the two analyses.

GSEA is a computational approach to determine if a pre-defined gene set can show a significantly consistent difference between two biological states.[19] To further understand the relevant signaling pathway events, we used Java GSEA (version 3.0) platform to analyze gene set enrichment. Gene sets were defined as those with statistically significant difference when only the nominal P values < 0.05 and false discovery rate values < 0.25.

Integration of Protein-Protein Interaction (PPI) Network and Module Analysis

STRING database is an online tool for assessment and integration of interactions of genes and proteins.[20] We used STRING to assess the interactional relationships among the DEGs, then used the Cytoscape 3.6.1 to build a PPI network. The plug-in Molecular Complex Detection (MCODE)

was utilized to screen the most significant module in the PPI networks according to the following criteria for selection: MCODE scores >10, degree cut-off=2, node score cut-off=0.2, Max depth=100 and k-score=2.

Real-time quantitative PCR

Total RNA was extracted from the spleen or retina using the TRIZOL reagent according to the manufacturer's protocols. The first-strand cDNA was generated by using PrimeScript™ RT Reagent Kit with gDNA Eraser (Takara, Dalian, China). The cDNA was quantified by Applied Biosystems 7500 Fast Real-Time PCR System (Applied Biosystems, Foster City, CA, USA). The primers of TNF-α, IL-6, IL-1β, CXCL2, MCP-1(CCL2), iNOS and Arg-1 are shown in Table e-1. The primers of INF-γ, IL-17, Foxp3 and IL-10 specific for mice were those designed according to the report previously described[9]. For human PGRN detection, the following primers were used: β-actin: forward, 5′-GGATGCAGAAGGAGATCACTG-3′, reverse, 5′-CGATCCACACGGAGTACTTG-3′; and PGRN: forward, 5′-ATGTGGGTCCTGATGAGCTG-3′, reverse,5′-GCTCGTTATTCTAGGCCATGTG-3′. Gene expression was normalized relative to the expression of β-actin or GAPDH.

Flow Cytometry Analysis

For intracellular cytokine staining, the cultured cells or the spleen cells from EAU/EAE mice were pulsed with ionomycin (1 ug/mL; Sigma) and PMA (100ng/mL; Sigma) for 5 h at 37°C. At 1 hour of culture, brefeldin A (10 ug /mL; Sigma) was added and cultured for 4h. The cells were then harvested and stained with cell surface marker anti-mouse CD4 antibody before fixation and permeabilization with Cytofix/Cytoperm kit (eBioscience, San Diego, CA, USA). The cells were finally stained with fluorescent antibodies including p-STAT5, anti-mouse IFN-γ, anti-mouse IL-17A, anti-mouse Foxp3 or anti-mouse CD25 for 30 minutes. Samples were analyzed on a FACSAria flow cytometer and analyzed using CellQuest software (BD Biosciences). The antibodies for intracellular analysis were all from Biolegend and BD Biosciences.

To verify the key signaling pathway enriched in the KEGG pathway and GSEA analysis by flow cytometry, splenocytes were harvested from WT EAU and $PGRN^{-/-}$ EAU mice. After

washing and resuspending, these cells were fixed and permeabilized using Fix/Perm cell permeabilization reagents, followed by incubation with fluorescently labeled antibodies against phospho-p38/JNK/ERK1/2 (Biolegend). Flow cytometric analysis was performed on FACSAria flow cytometer and data were analyzed with FlowJo software (Treestar, Ashland, OR).

Cytokine detection by Enzyme-Linked Immunosorbent Assay (ELISA)

Blood sample was collected from patients with active BD, active VKH and normal controls. After centrifugation, the serum was harvested and stored at −80°C. The levels of PGRN in the serum form patients and normal controls were measured using human progranulin quantikine ELISA kit (R&D systems).

Reference:

e1. Yang, P. *et al.* Clinical characteristics of Vogt-Koyanagi-Harada syndrome in Chinese patients. *Ophthalmology* **114**, 606-614 (2007).

e2. Du, L., Kijlstra, A. & Yang, P. Vogt-Koyanagi-Harada disease: Novel insights into pathophysiology, diagnosis and treatment. *Prog Retin Eye Res* **52**, 84-111 (2016).

e3. Criteria for diagnosis of Behcet's disease. International Study Group for Behcet's Disease. *Lancet* **335**, 1078-1080 (1990).

e4. Yang, P. *et al.* Development and Evaluation of Diagnostic Criteria for Vogt-Koyanagi-Harada Disease. *JAMA Ophthalmol* **136**, 1025-1031 (2018).

e5. Read, R.W. *et al.* Revised diagnostic criteria for Vogt-Koyanagi-Harada disease: report of an international committee on nomenclature. *Am J Ophthalmol* **131**, 647-652 (2001).

e6. Chen, Y. *et al.* Comparative Analysis of the Interphotoreceptor Retinoid Binding ProteinInduced Models of Experimental Autoimmune Uveitis in B10.RIII versus C57BL/6 Mice. *Curr Mol Med* **18**, 602-611 (2018).

e7. Huang, Y. *et al.* Aryl Hydrocarbon Receptor Regulates Apoptosis and Inflammation in a Murine Model of Experimental Autoimmune Uveitis. *Frontiers in immunology* **9**, 1713 (2018).

e8. Mattapallil, M.J. *et al.* Characterization of a New Epitope of IRBP That Induces Moderate to Severe Uveoretinitis in Mice With H-2b Haplotype. *Investigative ophthalmology & visual science* **56**, 5439-5449 (2015).

e9. Yang, H. *et al.* Activation of liver X receptor alleviates ocular inflammation in experimental autoimmune uveitis. *Investigative ophthalmology & visual science* **55**, 2795-2804 (2014).

e10. Zhao, Y.P. *et al.* Progranulin protects against osteoarthritis through interacting with TNF-alpha and beta-Catenin signalling. *Annals of the rheumatic diseases* **74**, 2244-2253 (2015).

e11. Song, Z. *et al.* Progranulin Plays a Central Role in Host Defense during Sepsis by Promoting Macrophage Recruitment. *American journal of respiratory and critical care medicine* **194**, 1219-1232 (2016).

e12. Cortes, L.M. *et al.* Repertoire analysis and new pathogenic epitopes of IRBP in C57BL/6 (H-2b) and B10.RIII (H-2r) mice. *Investigative ophthalmology & visual science* **49**, 1946-1956 (2008).

e13. Do, J. *et al.* Treg-specific IL-27Ralpha deletion uncovers a key role for IL-27 in Treg function to control autoimmunity. *Proc Natl Acad Sci U S A* **114**, 10190-10195 (2017).

e14. Wang, L.M. *et al.* Nr4a1 plays a crucial modulatory role in Th1/Th17 cell responses and CNS autoimmunity. *Brain Behav Immun* **68**, 44-55 (2018).

e15. Love, M.I., Huber, W. & Anders, S. Moderated estimation of fold change and dispersion for RNA-seq data with DESeq2. *Genome Biol* **15**, 550 (2014).

e16. The Gene Ontology (GO) project in 2006. *Nucleic Acids Res* **34**, D322-326 (2006).

e17. Kanehisa, M. & Goto, S. KEGG: kyoto encyclopedia of genes and genomes. *Nucleic Acids Res* **28**, 27-30 (2000).

e18. Huang, D.W. *et al.* DAVID Bioinformatics Resources: expanded annotation database and novel algorithms to better extract biology from large gene lists. *Nucleic Acids Res* **35**, W169-175 (2007).

e19. Subramanian, A. *et al.* Gene set enrichment analysis: a knowledge-based approach for interpreting genome-wide expression profiles. *Proc Natl Acad Sci U S A* **102**, 15545-15550 (2005).

e20. Szklarczyk, D. *et al.* STRING v10: protein-protein interaction networks, integrated over the tree of life. *Nucleic Acids Res* **43**, D447-452 (2015).